Supplementary Information

3D-Printed Pre-filter with Crystal Violet–Gold Nanocluster Hybrid for Reusable Visible-Light-Activated Antimicrobial Air Filtration

Jae Hak Shin[1,†], So Yeong Kim[2,†], Hyun Sung Kang[2], In Ho Kim[1], Joon Young Park[1], Ki Joon Heo[2], Gi Byoung Hwang[3,4*], Jae Hee Jung[1,5*]*

[1] Department of Mechanical Engineering, Sejong University, Seoul 05006, Republic of Korea
[2] School of Mechanical Engineering, Chonnam National University, Gwangju 61186, Republic of Korea
[3] Department of Chemistry, University College London, London, WC1H 0AJ, United Kingdom
[4] Lab.M.0, Seoul 04799, Republic of Korea
[5] Department of Aerospace System Engineering, Sejong University, Seoul 05006, Republic of Korea

[†] These authors contributed equally to this work.
* Corresponding authors
E-mail address: k.heo@jnu.ac.kr (Ki Joon Heo), gi-byoung.hwang.14@ucl.ac.uk (Gi Byoung Hwang), jaehee@sejong.ac.kr (Jae Hee Jung)

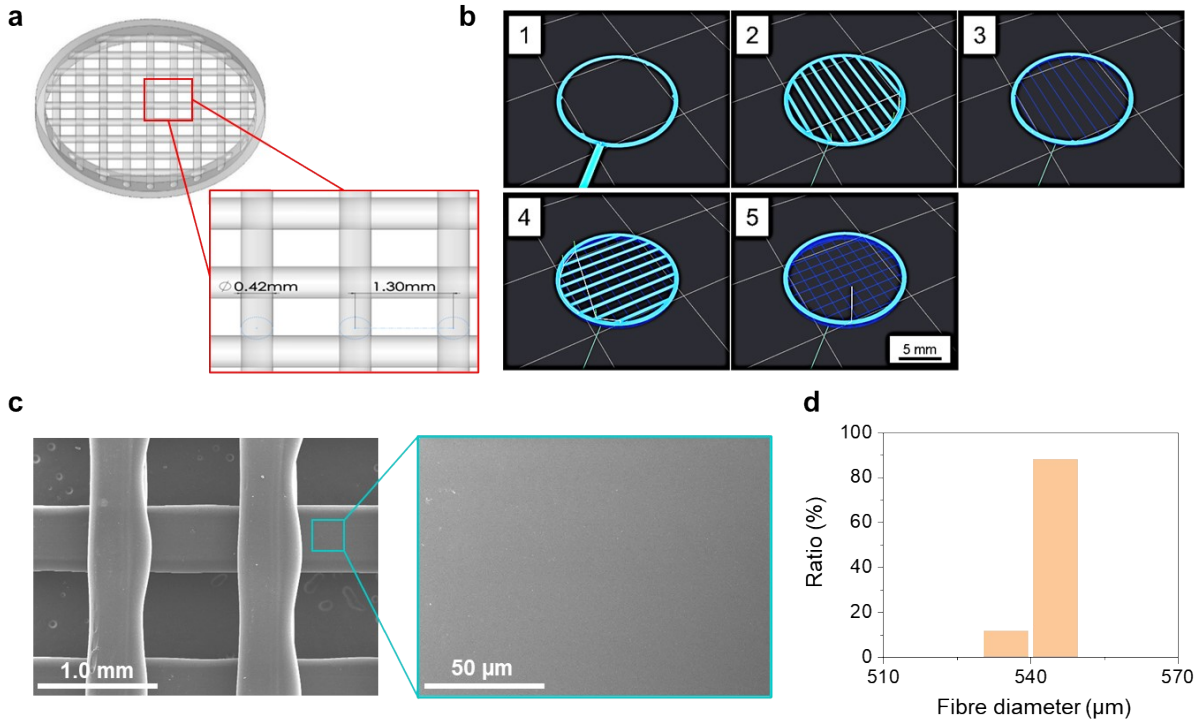

Figure S1. (a) CAD schematic of the pre-filter. (b) Simulated 3D printing path illustrating the layer-by-layer deposition sequence of the pre-filter. (c) SEM image of the printed pre-filter. (d) Distribution of fibre diameter through microscopic image analysis of the manufactured TPU pre-filter.

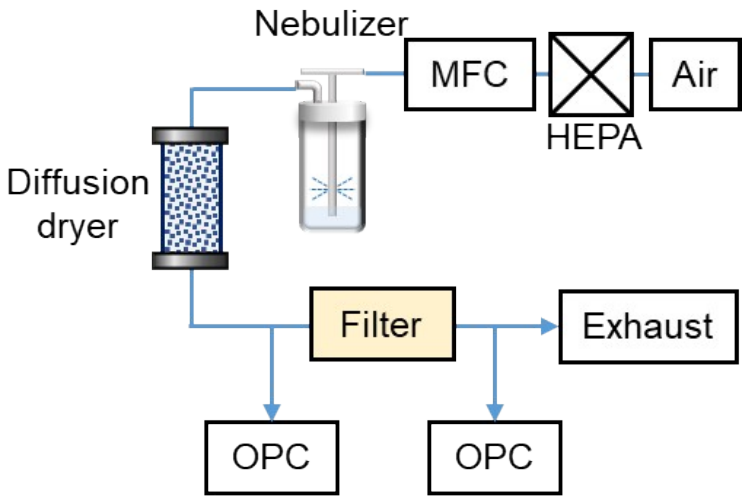

Figure S2. Experimental setup for filtration performance test using *S. epidermidis* bioaerosols.

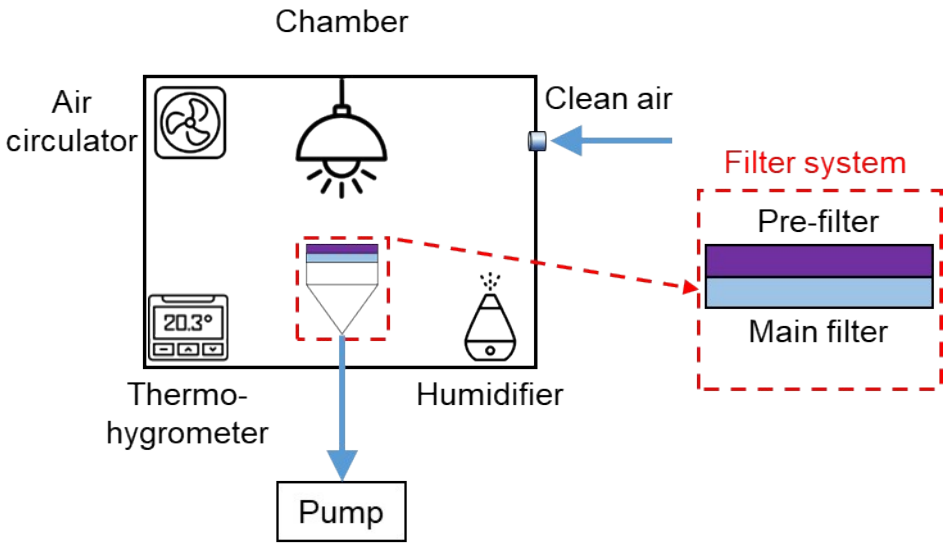

Figure S3. Schematic illustration of airflow-assisted antibacterial testing setup of antimicrobial air filter system under various face velocities.

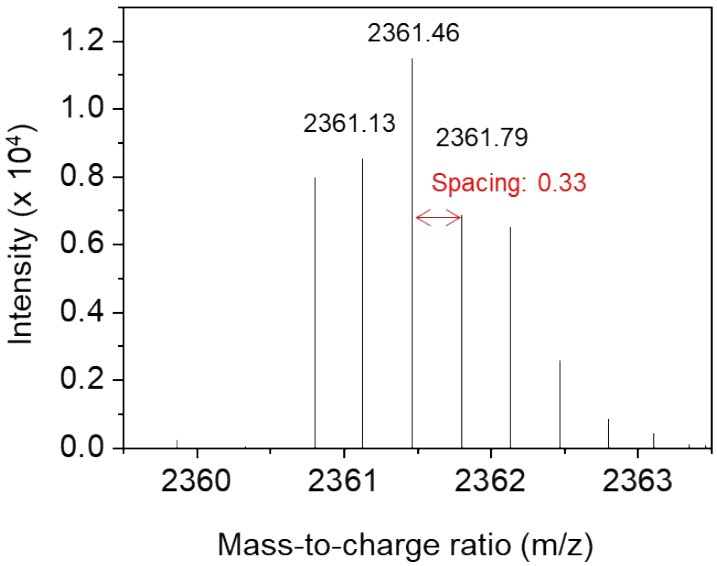

Figure S4. Enlarged experimental isotope pattern of peak #1 in Figure 2c showing 0.33 spacing between ^{12}C and ^{13}C.

Table S1. Theoretical and experimental characteristic peak positions of $[Au_{25}(Cys)_{18}]$ under ESI-MS, with corresponding empirical formulations of gas-phase ions.

Peak number	Characteristic peak position (m/z)		Empirical formulations of gas-phase ions formed under ESI	Exact mass (Da)
	Theoretical	Experimental		
#1	2361.43	2361.46	$[Au_{25}(Cys)_{18}\text{-}3H^{+}]^{3-}$	7084.38
#2	2368.08	2368.13	$[Au_{25}(Cys)_{18}\text{-}4H+Na]^{3-}$	7104.39
#3	2375.44	2376.12	$[Au_{25}(Cys)_{18}\text{-}5H+2Na]^{3-}$	7128.36
#4	2382.74	2382.75	$[Au_{25}(Cys)_{18}\text{-}6H+3Na]^{3-}$	7148.25
#5	2390.08	2390.46	$[Au_{25}(Cys)_{18}\text{-}7H+4Na]^{3-}$	7171.38
#6	2397.42	2397.31	$[Au_{25}(Cys)_{18}\text{-}8H+5Na]^{3-}$	7191.93

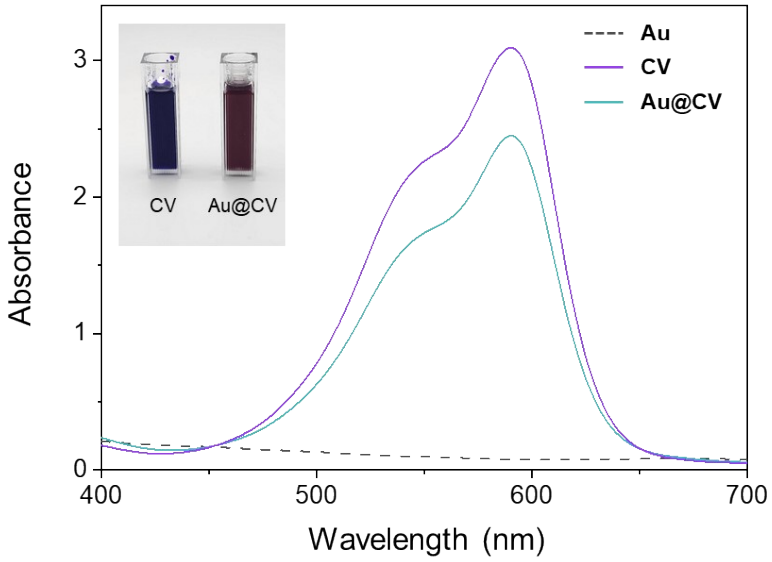

UV-vis absorbance spectra of only Au, only CV, and Au@CV-coated TPU film

Figure S5. UV-vis absorbance spectra of TPU pre-filters coated with Au, CV, and Au@CV. Inset: digital images of CV and Au@CV solutions.

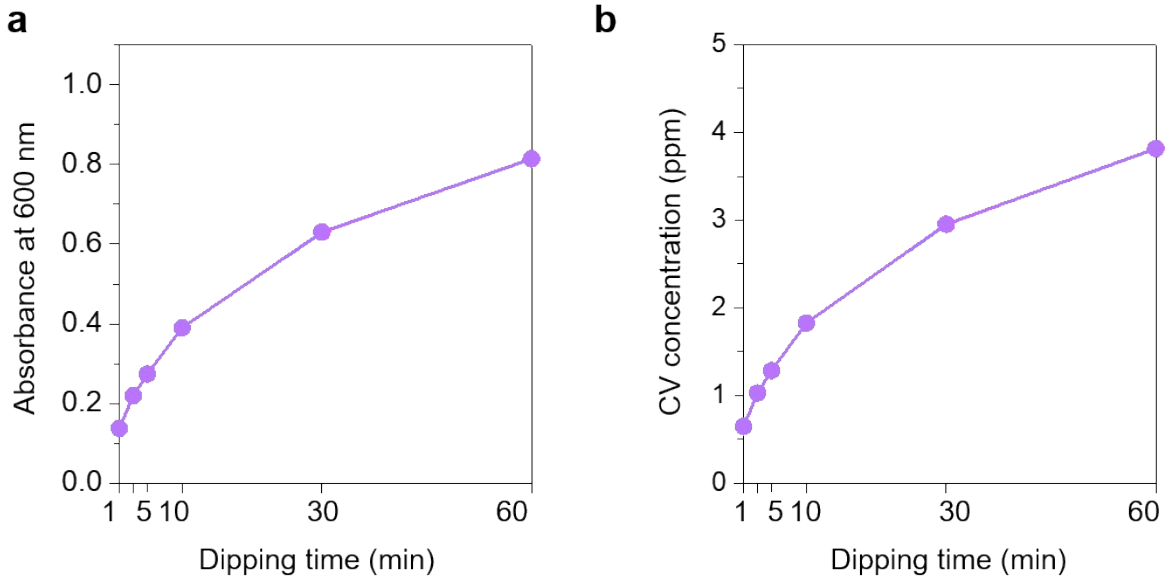

Figure S6. (a) Absorbance at 600 nm of Au@CV-coated TPU film as a function of coating time. (b) The total coating amount (ppm) of CV determined from UV-vis calibration. For this measurement, a flat TPU film with the same polymer composition was used instead of the porous pre-filter employed in the paper.

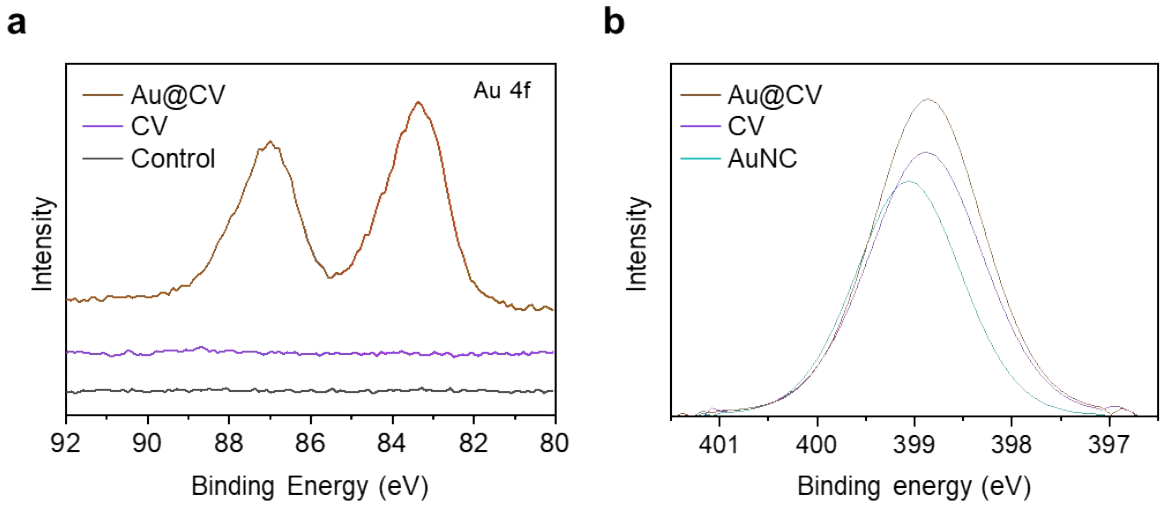

Figure S7. (a) XPS Au 4f spectra of control, CV-coated, and Au@CV-coated pre-filters. (b) N 1s spectra of CV only, AuNC only, and Au@CV filter. The C 1s peak at 285.8 eV was used as the internal energy reference.

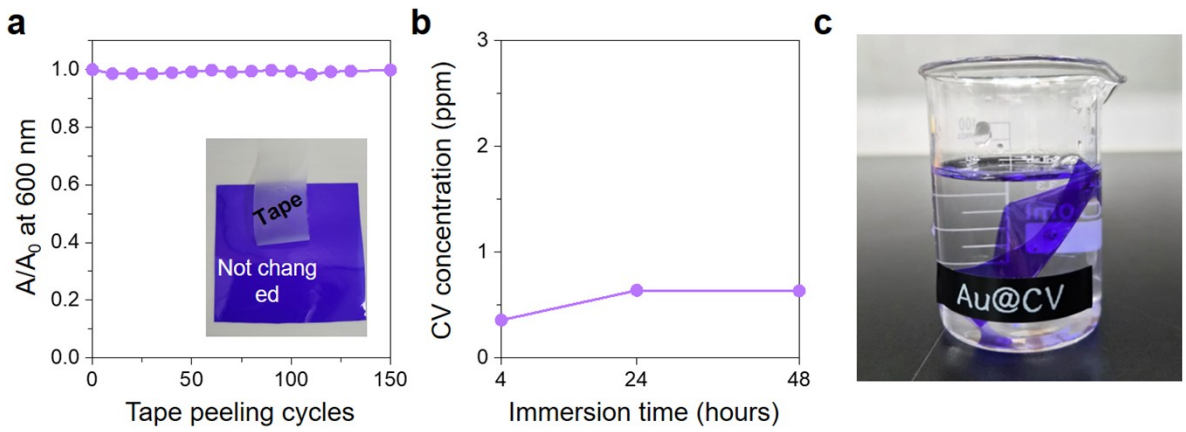

Figure S8. (a) Adhesive tape peeling test of the Au@CV-coated film (coating time: 24 h). A new piece of Sellotape was applied and removed for each peeling cycle. A and A_0 represent the absorbance at 600 nm after peeling (A) and before peeling (initial, A_0), respectively. (b) Leaching of CV from the Au@CV surface. The Au@CV films were cut into 3 x 3 cm portions and dipped into deionized water for 48 hours. (c) Photograph of the Au@CV-coated TPU film immersed in deionized water.

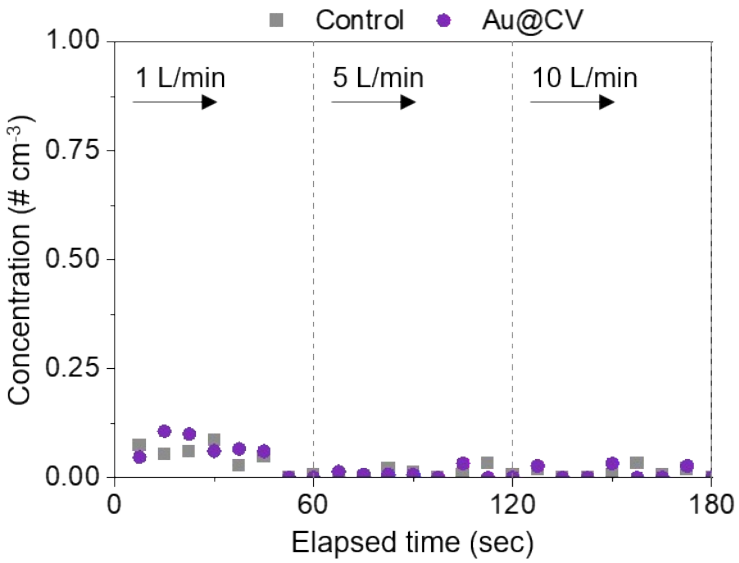

Figure S9. The particle number concentration was measured downstream of the control and Au@CV pre-filter at various flow rates. We examine the possible surface detachment or structural degradation of the Au@CV filter under airflow conditions. The residual particles released from the Au@CV pre-filter were measured using a condensation particle counter (CPC, Model 3750, TSI Inc.), which can detect particles larger than 7 nm. The Au@CV pre-filter was mounted in a sealed filter holder, and particle number concentrations downstream of the filter were continuously monitored under clean-air flow. The background signal from an empty filter holder (Control) was recorded under identical conditions for comparison.

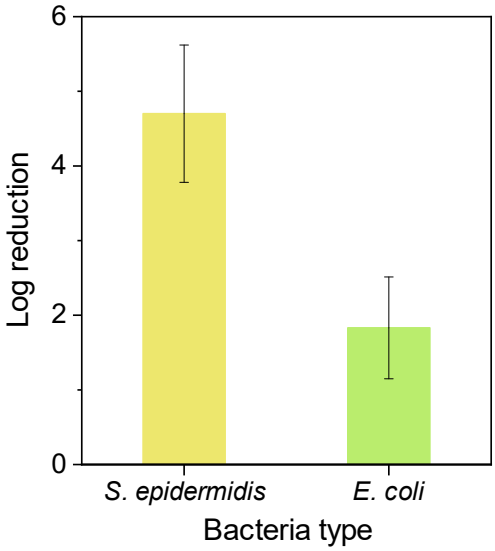

Figure S10. Photobactericidal activity against Gram-positive (*S. epidermidis*) and Gram-negative (*E. coli*) bacteria at 11.9 mW cm-2 for 3 h.

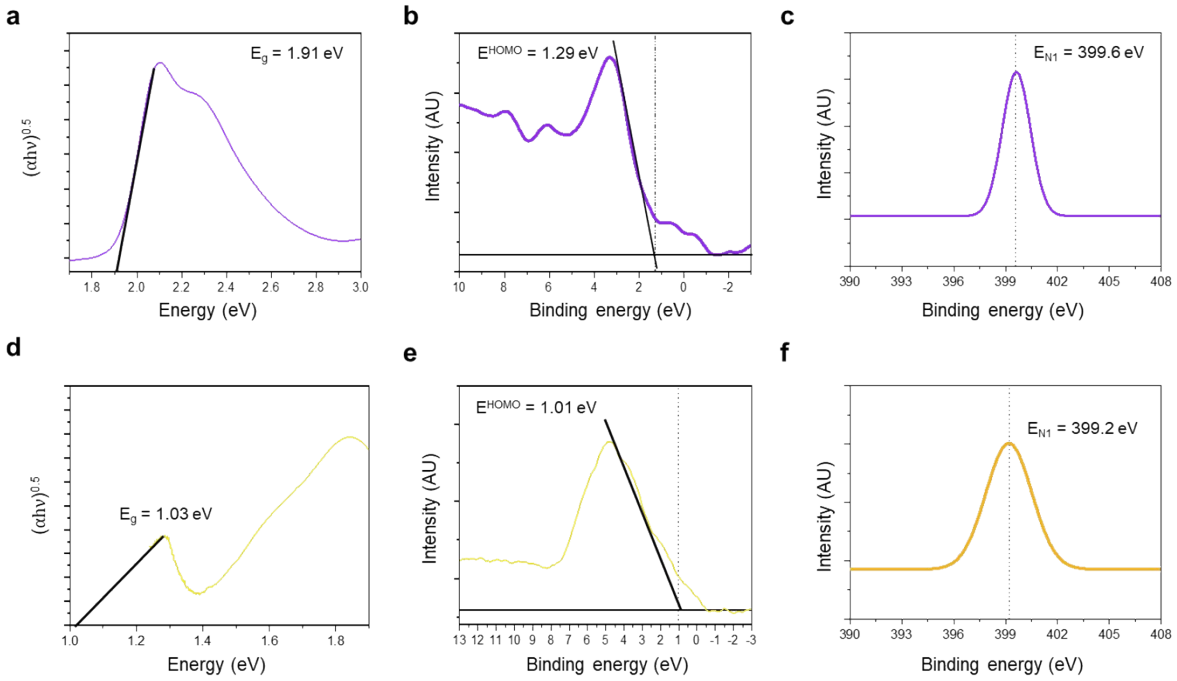

Figure S11. (a) Band gap, (b) HOMO band, and (c) N 1s spectra for CV. (d) Band gap, (e) HOMO band, and (f) N 1s spectra for AuNC.

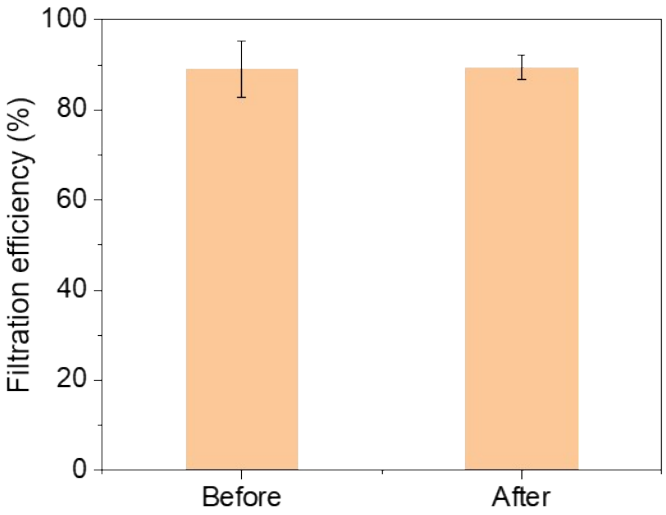

Figure S12. The filtration efficiency of the main filter measured before and after continuous exposure to ROS from the Au@CV pre-filter.

To evaluate the effect of ROS exposure on the main filter performance, the same experimental setup as in the airflow-assisted antibacterial test (Figure S3) was employed. The filter was irradiated with visible light for 3 h under continuous airflow (2.4 cm s^{-1}), and the filtration efficiency of the main filter was measured before and after exposure using an optical particle counter.